Available online at www.sciencedirect.com

SCIENCE DIRECT®

Journal of volcanology and geothermal research

ELSEVIER

Journal of Volcanology and Geothermal Research 146 (2005) 102–116

www.elsevier.com/locate/jvolgeores

A satellite chronology of the May–June 2003 eruption of Anatahan volcano

Robert Wright[a,*], Simon A. Carn[b], Luke P. Flynn[a]

[a]*Hawaii Institute of Geophysics and Planetology, University of Hawaii, 1680 East-West Road, Honolulu, HI 96822, USA*
[b]*Joint Center for Earth Systems Technology (NASA/UMBC), University of Maryland Baltimore County, 1000 Hilltop Circle, Baltimore, MD 21250, USA*

Received 21 July 2004; accepted 26 October 2004

Abstract

The first recorded eruption of Anatahan began at approximately 17:00 local time on May 10, 2003. Here, we present observations made by a suite of Earth-orbiting satellites of the heat, ash and gas emitted from the volcano before, during and after the eruption. No thermal or sulphur dioxide emissions are apparent in MODIS (Moderate Resolution Imaging Spectroradiometer), AIRS (Atmospheric Infrared Sounder), EP TOMS (Earth Probe Total Ozone Mapping Spectrometer) and ASTER (Advanced Spaceborne Thermal Emission and Reflection Radiometer) satellite images acquired prior to the eruption. However, within 24 h of eruption onset, the University of Hawaii's near-real-time satellite thermal monitoring system 'MODVOLC' detected the eruption and confirmed Anatahan's eastern caldera as the center of the activity. Although the eruption was initially phreatic, it quickly transitioned into a magmatic phase that culminated in the emplacement of a dacitic lava dome. The onset of the magmatic phase is recorded by MODVOLC as an order of magnitude increase in the heat flux from the volcano after May 16, indicative of fresh lava at the surface, relative to low values (50–90 MW) observed during the initial phreatic phase. MODVOLC detected thermal emission from the volcano on a further 22 occasions during the next 2 weeks, allowing us to quantitatively document temporal variations in thermal output during the eruption.

We use MODIS, EP TOMS and AIRS data to document ash and sulphur dioxide emissions from Anatahan covering the period May 10–June 13, 2003. Using daily satellite observations in conjunction with ground-based estimates, we arrive at a total SO_2 discharge of ~0.51 Mt for the ~1 month of activity, of which ~0.11 Mt was emitted during activity on May 10–12. Decreases in measured SO_2 flux prior to the observation of a lava dome on June 4 indicate that the emerging dome may have blocked the upper conduit and inhibited degassing during this period.

A new episode of dome growth was detected by MODVOLC on April 12, 2004. So far, the level of thermal emission during the recent period of activity is substantially lower than that observed during the May–June 2003 eruption.
© 2005 Elsevier B.V. All rights reserved.

Keywords: Anatahan; remote sensing; MODIS; TOMS; ash; SO_2

* Corresponding author. Tel.: +1 808 956 9194; fax: +1 808 956 6322.
E-mail address: wright@higp.hawaii.edu (R. Wright).

0377-0273/$ - see front matter © 2005 Elsevier B.V. All rights reserved.
doi:10.1016/j.jvolgeores.2004.10.021

1. Introduction

The first historic eruption of Anatahan, in the northern Mariana Islands (145.70°E, 16.34°N), began on May 10, 2003. Anatahan is an elongated, 9-km-long island composed of two coalescing volcanoes, calderas at the summits of which overlap to produce a 2×5 km east–west-trending depression in the center of the island (Fig. 1A).

The remote location of the volcano, the absence of a resident population and a lack of geophysical instrumentation meant that the onset of the eruption went largely unnoticed. Although a seismometer had been installed on May 6, 4 days prior to the start of the eruption, the data were not being telemetered and the first direct confirmation that an eruption was taking place came when an ash plume was observed from the research ship *MV Super Emerald*, on the morning of May 11 (Smithsonian Institution, 2003a). Seismic records indicate that the eruption in fact began at around 16:20 on May 10, when, after several hours of intermittent seismicity, a period of near-continuous earthquake activity began (Pozgay et al., 2003). Although geographically remote, eruption plumes of up to 12 km altitude meant that the eruption posed a hazard to trans-Pacific aircraft, prompting the Washington Volcanic Ash Advisory Center (VAAC) to issue an advisory to the aviation community at 23:00 on May 10 (all times local: Greenwich Mean Time+10), after ash clouds were observed in GOES weather satellite images (Smithsonian Institution, 2003a).

The eruption was initially phreatic with explosions ejecting ash, which was dispersed across the entire

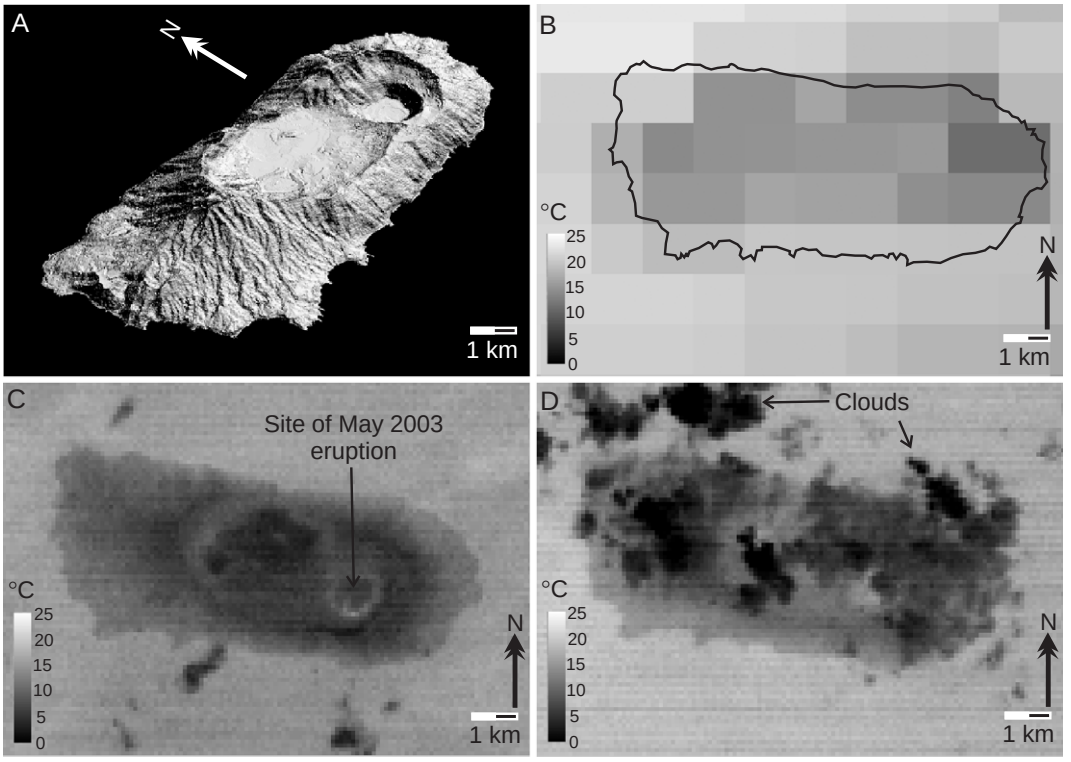

Fig. 1. (A) Perspective view, shaded relief representation of the topography of Anatahan. (B) Terra MODIS nighttime image of Anatahan, acquired at 22:55 (all times local: Greenwich Mean Time+10.00) on May 5, 2003, 5 days prior to the beginning of the eruption. Spectral radiance data acquired at 3.959 μm (MODIS band 22) have been converted to brightness temperature, in °C. Pixel size is 1 km and the outline of the island is superimposed. (C, D) Nighttime ASTER images acquired at 22:45 on June 11, 2001 and 22:37 on October 4, 2002, respectively. In each instance, spectral radiance data at 11.318 μm (ASTER band 14) have been converted to brightness temperature, in °C. Pixel size is 90 m. The eastern crater, site of the May 2003 eruption and ongoing (at the time of this submission) activity, is marked.

island, and bombs (some up to several meters in diameter), which mainly fell back in the near-vent region (Smithsonian Institution, 2003a). The eruptive vent, sited in Anatahan's eastern crater, continued to produce ash plumes throughout May 2003, although most failed to exceed a height of 6 km (Smithsonian Institution, 2003a). Lava, in the form of a small, spiny dome, was first observed in the eastern crater on June 4, 2003. However, the high SO_2 fluxes (3500–4000 t day^{-1}) measured using ship-based COSPEC (Correlation Spectrometer) on May 21, combined with analysis of a sequence of eruption deposits on the western side of the island, indicate that the eruption had entered its magmatic phase prior to this observation (Fischer et al., 2003). Much of this small dome was destroyed by two explosions that took place on June 14 (Smithsonian Institution, 2003b). Seismic and volcanic activity declined after June 16 (Smithsonian Institution, 2003b), and by mid-July only emissions of steam were observed from the eruption site.

Satellite sensors are ideal for detecting and monitoring eruptions that take place at remote and poorly instrumented volcanoes such as Anatahan. This is particularly true if the data are collected routinely and are processed and analyzed in near-real-time. Until relatively recently, the timely reception, processing and analysis of many satellite data sets was hindered by limits to the computing power available to process them and the lack of sufficient bandwidth for transferring the large volumes of data quickly. However, high-speed data transfer, the proliferation of powerful desk-top computers, and the ability and willingness of satellite data providers to make their data available in a timely manner (and at a reasonable cost), has meant that satellite data are increasingly being incorporated into autonomous analysis systems. Even if the data analysis is not fully automated, the time interval between satellite acquisition and delivery of a useable product to the analyst is now sufficiently short (i.e., a matter of hours) that satellite data can be used to provide quantitative volcanic eruption parameters, as well as basic information regarding the nature and distribution of the erupted products. This is of importance to hazard mitigation officials who require data in near-real-time to aid in disaster assessments.

Here, we present a suite of satellite observations compiled using data from the Moderate Resolution Imaging Spectroradiometer (MODIS), the Earth Probe Total Ozone Mapping Spectrometer (EP TOMS) and the Atmospheric Infrared Sounder (AIRS), that document how emissions of heat, ash and sulphur dioxide varied during the May 2003 eruption of Anatahan. Thermal emission from the volcano is characterized using NASA's MODIS instrument. MODIS acquires spectral radiance data at both the short- and long-wave infrared wavelengths, and is ideally suited to detecting and quantifying the heat emitted by active lava flows, lava domes, lava lakes and erupting vents (Wright and Flynn, 2004). The spectral resolution of MODIS is also appropriate for detecting the presence of volcanic ash in the atmosphere (Watson et al., 2004) as well as determining the amount of sulphur dioxide emitted during passive and explosive degassing events (Watson et al., 2004), while TOMS has been used since 1978 to document global volcanic SO_2 emissions (Carn et al., 2003), particularly during explosive eruptions. It has recently been demonstrated that the AIRS sensor, flown on-board NASA's Aqua satellite, can also detect the presence of SO_2 and volcanic ash in the atmosphere (Carn et al., 2005).

Using these data sets, we have compiled a satellite chronology of heat, gas and particulate emissions from the first recorded eruption at this remote volcano.

2. Satellite observations of Anatahan prior to May 10, 2003

Pozgay et al. (2003) report that the only significant "precursory" earthquake activity involved an earthquake swarm about 15 km distant from the volcano, at a depth much greater than the earthquakes subsequently observed during the eruption, while scientists who visited the island on May 6 to deploy a seismometer found no sign of the impending eruption. Likewise, we have found no evidence for eruption precursors, thermal or otherwise, in the satellite data we have inspected.

Although the May 2003 eruption was the first recorded at Anatahan, seismic unrest has occurred recently, the island being evacuated in April 1990 in response to a series of shallow earthquakes 5 to 38 km from the island (Smithsonian Institution, 1990).

Although no eruption occurred at this time, apparent increases in the thermal activity of the eastern crater-lake and fumaroles were noted (Smithsonian Institution, 1990), as was the presence of hot springs and boiling mud pools.

MODIS acquires infrared radiance data in the short- and long-wave regions of the electromagnetic spectrum and is appropriate for detecting geothermal heat sources at the Earth's surface. Two MODIS sensors are currently in orbit, one carried on-board NASA's Terra platform and the other on Terra's sister-ship, Aqua. In each 24-h period, 576 MODIS images are acquired, each covering an area of approximately 1354×2030 km, providing complete global coverage. The MODVOLC system (Wright et al., 2002a, 2004) analyses every pixel within each of these images for the presence of pixel- and sub-pixel-sized high-temperature heat sources at the Earth's surface. If the thermal signature of a volcanic "hot-spot" is detected, i.e., an active lava flow, dome, lake or vent, its properties are recorded and reported on the internet. Typically, there is an 8–12 h delay between satellite overpass and the results becoming available. As the algorithm routinely analyses every square kilometer of the Earth's surface, at least once in any given 24-h period, the system is able to detect eruptions when and where they are least "expected". As a result, within 24 h of the eruption onset, the presence of active lava at the surface of Anatahan was reported at the following http://modis.higp.hawaii.edu. However, MODVOLC only began to detect elevated surface temperatures at Anatahan after the eruption began.

In order to establish whether there were any thermal precursors to the eruption that fell below the detection limit of this algorithm, for example, increases in fumarolic activity or the temperature of the crater-lake, we manually inspected 53 nighttime MODIS images acquired in the month before the eruption began. Nighttime images provide the best opportunity for resolving subtle temperature anomalies, as any geothermal signal will be uncontaminated by the effects of solar heating and, in the case of MODIS, reflected sunlight. No thermal precursors were apparent.

Given the coarse spatial resolution of the MODIS data (MODIS pixels are, at best, 1 km on a side; Fig. 1b), this is perhaps not surprising: low-temperature manifestations of active volcanism, such as fumarolic activity, are relatively difficult to detect, particularly in low-spatial-resolution data (see Rothery et al., 1995 for a discussion). However, high-spatial-resolution instruments, such as the Landsat 7 ETM+ (Enhanced Thematic Mapper Plus; Flynn et al., 2001) and the Terra ASTER (Advanced Spaceborne Thermal Emission and Reflection Radiometer; Pieri and Abrams, 2004), acquire data at the long-wave infrared wavelengths (i.e., 8–14 μm) appropriate for detecting low-temperature geothermal heat, and given their small pixel size (60 and 90 m, respectively), provide more opportunity for detecting changes in the kind of low temperature thermal activity reported to exist at Anatahan in the 1990s.

Unfortunately, such sensors do not acquire data for all of Earth's volcanoes routinely, and their relatively low revisit frequency (both ASTER and ETM+ pass over Anatahan once every 16 days) means that an extended cloud-free satellite time-series is difficult to acquire and monitoring baselines difficult to establish. In the 3 years prior to the May 2003 eruption, only two nighttime ASTER scenes of Anatahan were acquired, while no nighttime ETM+ data exist. Fig. 1 shows both of the available nighttime ASTER images, acquired on June 11, 2001 and October 4, 2002. Here, the raw spectral radiance data have been converted to temperature, where increasing pixel brightness corresponds to increasing surface temperature.

On June 11, 2001, a cluster of ASTER pixels on the southern rim of the eastern crater has a temperature ~2 °C higher than its immediate neighbours (Fig. 1c). Pixels on the rim of the western crater, which was not involved in the 2003 eruption, also have slightly elevated temperatures, albeit by only ~0.5 °C. Although the pixels on the rim of the eastern crater appear "anomalously" warm, their location, which lies away from the main center of fumarolic activity at the bottom of the crater, combined with the fact that pixels on the rim of the western crater also appear to have slightly elevated temperature, indicates that this is almost certainly a residual solar heating effect (the image was acquired ~4 h after sunset) and not a geothermal anomaly. This interpretation is reinforced by inspection of the October 4, 2002 image (Fig. 1d). On this date, the rim of the eastern crater was also warmer

than the surrounding ground surface, again by ~2 °C. However, once more, the rim of the western crater shows a similar thermal "anomaly".

The significance of apparent spatio-temporal changes in surface temperature at potentially active volcanoes can only be determined if an extended time-series of data is available for comparison. With such an incomplete high spatio-temporal resolution baseline, it is impossible to determine whether any significant changes in the temperature of the eastern

Table 1
Satellite observations of SO_2 and ash emissions from Anatahan, May–June 2003

Date and time	Sensor	Observations
10 May–2310	Terra MODIS	Detached SO_2 cloud (~14 kt) bounded by 145°E–147°E and 13.5°N–16°N. Attached ash cloud extending S to 14°N and W to 144°E.
11 May–0155	Aqua MODIS	Detached SO_2 cloud (~11 kt) bounded by 145°E–146.5°E and 14°N–16°N. Attached ash cloud extending S to 14.5°N and thicker ash spreading W beyond 144°E.
11 May–0155	AIRS	Detached SO_2 cloud (~34 kt) bounded by 145°E–148°E and 12.5°N–16°N. Attached ash cloud (~1300 kt) extending S to 13°N and spreading W to 143°E.
11 May–1027	EP TOMS	Data gap over Anatahan. Narrow SO_2 cloud (~10 kt) between 147.5°E[a] and 152°E. Small, detached ash cloud at 14.5°N, 150°E.
11 May–1125	Terra MODIS	Detached SO_2 cloud (~16 kt) extending E of 144.5°E between 12°N and 14.5°N. Attached ash cloud extending W to 142°E and NW to 18°N.
11 May–1245	Aqua MODIS	Narrow SO_2 cloud (~21 kt) bounded by 148°E[a]–154°E and 12.7°N–17.1°N.
11 May–1245	AIRS	Narrow SO_2 cloud bounded by 150.6°E[a]–157.1°E and 12.5°N–15°N.
11 May–2215	Terra MODIS	Detached ash cloud bounded by 140°E–145°E and 15°N–17.5°N.
12 May–0100	AIRS	Weak SO_2 cloud bounded by 160.3°E–163.2°E and 17.5°N–18.5°N.
12 May–0240	Aqua MODIS	Detached ash cloud bounded by 139°E–144°E and 15.5°N–18°N.
12 May–0240	AIRS	Detached, weak SO_2 cloud extending from 140.8°E–143.6°E[a] between 14.2°N[a] and 17.4°N. Detached ash cloud extending from 137.1°E–143.6°E[a] between 14.2°N[a] and 17.9°N.
12 May–1030	Terra MODIS	Detached ash cloud W of 143°E between 16°N and 18.5°N.
12 May–1115	EP TOMS	Detached, elongate SO_2 cloud (~99 kt) bounded by 140°E–150°E and 11°N–16°N. Detached ash cloud centered at 17°N, 140°E.
12 May–1330	Aqua MODIS	Detached, diffuse ash cloud bounded by 138°E–142°E and 15.5°N–18.5°N.
12 May–1330	AIRS	Detached, elongate SO_2 cloud bounded by 140°E–157°E[a] and 10.5°N–15°N. Detached ash cloud bounded by 138.6°E[a]–143°E and 14.6°N–18.8°N.
13 May–0142	AIRS	Weak ash cloud signal W of 142°E between 16.8°N and 18.1°N.
13 May–1204	EP TOMS	Weak ash cloud signal between 135°E and 142°E.
13 May–1412	AIRS	Weak ash cloud signals bounded by 134°E–140.7°E and 15°N–19.2°N, and by 127.6°E[a]–129.7°E and 16.3°N–18.4°N.
14 May–0224	AIRS	Weak ash cloud signal bounded by 133°E–137.5°E and 15°N–18.5°N.
14 May–1115	EP TOMS	Weak attached SO_2 plume extending W to 140°E.
15–23 May	EP TOMS not operational	
24 May–1114	EP TOMS	SO_2 plume (~19 kt) extending SSE–SE from Anatahan.
25 May–1024	EP TOMS	Data gap over Anatahan. Narrow SO_2 plume (~23 kt) between 147.5°E and 153°E.
26 May–1114	EP TOMS	SO_2 plume (~35 kt) extending E from Anatahan.
28 May–1114	EP TOMS	SO_2 plume (~70 kt) extending NW from Anatahan.
30 May–1113	EP TOMS	SO_2 plume (~100 kt) extending NW from Anatahan.
03 June–1113	EP TOMS	SO_2 plume (~16 kt) extending SSW from Anatahan.
05 June–1113	EP TOMS	Weak SO_2 plume (<5 kt) extending W from Anatahan.
07 June–1112	EP TOMS	SO_2 plume (~7 kt) extending WNW from Anatahan.
09 June–1112	EP TOMS	SO_2 plume (~14 kt) extending NNW from Anatahan.
11 June–1112	EP TOMS	SO_2 plume (~15 kt) extending WSW from Anatahan.
13 June–1112	EP TOMS	SO_2 plume (~17 kt) extending WNW from Anatahan.

[a] Denotes edge of data granule, i.e., ash/SO_2 may extend further.

crater occurred prior to the May 2003 eruption. No SO_2 signals were apparent in satellite images acquired prior to eruption onset (Table 1).

3. The May–June 2003 eruption of Anatahan

3.1. Satellite observations of volcanic thermal emissions during the eruption

Direct confirmation that the eastern crater was the site of the eruptive activity was not possible until May 19, during a helicopter over-flight (Fischer et al., 2003). However, at 01:54 on 11 May, MODIS detected two hot-spots on the eastern flank of the east cone; 20 h later, another hot-spot was detected at the bottom of the eastern crater; 24 h later, at 01:44 on May 13, another two hot-spots were detected, again, within the eastern crater (Fig. 2). The geodetic location of the center-point of MODIS pixels is known to within ±50 m at the sub-satellite point (Wolfe et al., 2002). The hot-spots could, of course, be located anywhere within the 1-km instantaneous field of view of the sensor, approximated as the square box in the bottom right hand corner of Fig. 2. Furthermore, we have observed that, for some volcanic hot-spots that occupy fixed locations, such as the lava dome at Popocatepétl, the MODVOLC reported location of the hot-spot can vary by as much as ±1 km from the actual location. This uncertainty is approximated in Fig. 2 as the white open circle in the bottom right hand corner. Despite this, the geo-location accuracy of the hot-spots was still sufficient, combined with the near-real-time operation of the MODVOLC system, to allow the eastern crater to be identified as the source of the eruption within 48 h. MODVOLC detected hot-spots on a further 19 occasions during May 2003. Fig. 3A shows how they were heavily concentrated in and around the eastern crater. One hot-spot is located at the edge of the western caldera and we speculate that this represents a vegetation fire ignited by falling bombs.

Fig. 3B shows how the heat radiated from the Anatahan's eastern caldera varied during the course of

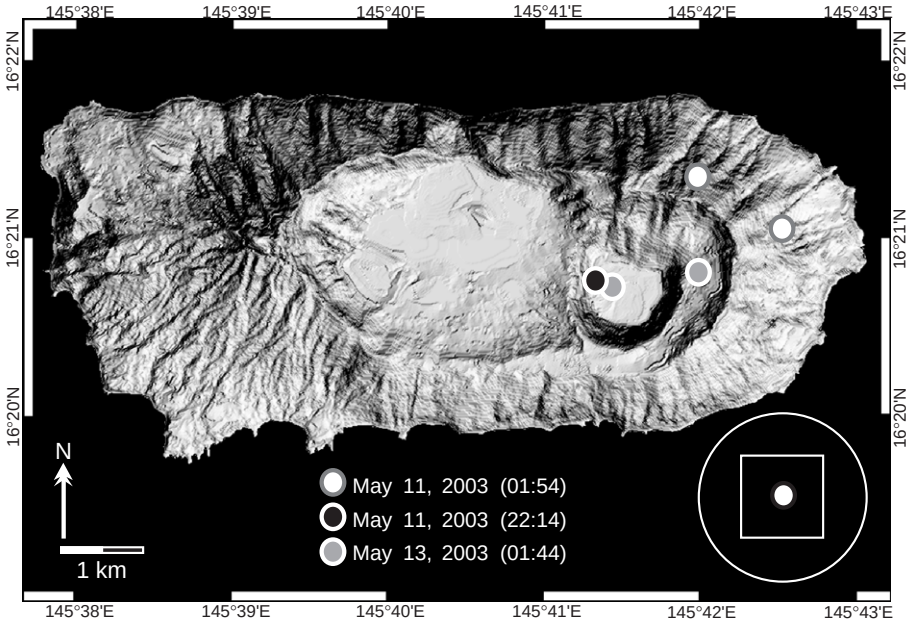

Fig. 2. The location of hot-spots detected by MODIS on May 11 and 13, 2003. Each filled circle denotes the geodetic location of the center-point of the MODIS pixel identified by the MODVOLC algorithm as containing a high-temperature heat source. The box in the bottom right corner shows the nominal size of the MODIS pixels (1 km at satellite nadir for the emissive channels used in this study) at this scale. The circle illustrates the potential error in the reported center-point, based on an analysis of the variation in the MODIS-recorded position of hot-spots at other volcanoes, which were in fact known to be spatially fixed (Wright et al., 2004).

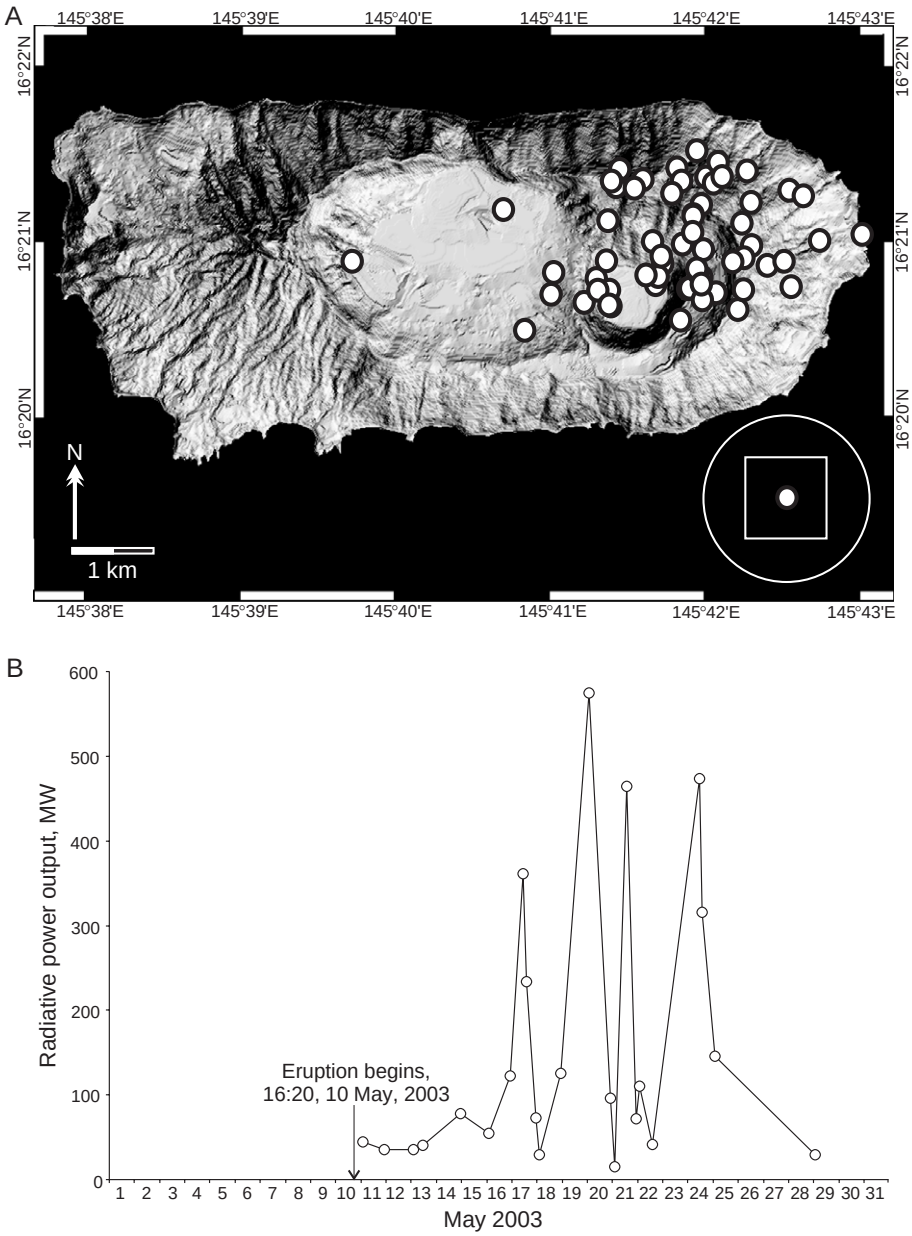

Fig. 3. (A) The spatial distribution of hot–spots detected by MODIS during the period May 11 to May 29, 2003. Each filled white circle corresponds to the center-point of the 1-km MODIS pixel that contained the hot-spot. (B) The total heat radiated in MW by these hot-spots over the same time period. Each data point represents the total heat estimated from all hot-spot pixels recorded at each discrete observation time.

the eruption, calculated from the MODIS spectral radiance data using the techniques described by Wright and Flynn (2004), and in Appendix A. Thermal output shows a waxing and waning trend, reaching a maximum value around May 20, either side of which the thermal emission curve is roughly symmetric. The coarse spatial resolution of the data means that the effects that volcanic ash and meteorological clouds may have on the detection process, for example, by obscuring all or part of the eruption site,

cannot be quantified. As a result, large decreases in the estimated thermal output on May 18, 20 and 22 depicted in Fig. 3B do not necessarily indicate hiatuses in the amount of heat the volcano was actually emitting. However, we have found that the general trends imparted by these MODIS-derived thermal emission time-series are representative of general fluctuations in the intensity of magmatic activity at many different volcanoes (e.g., Wright et al., 2002a, 2004; Wright and Flynn, 2004; Wright and Flynn, 2003).

Thermal emission from the eruption site during the period 01:54 on May 11 to 11:09 on May 13 (the first four MODIS hot-spot observations; Fig. 3B) occurred at a relatively low level, approximately 50 MW. This period of time corresponds to the initial phreatic phase of the eruption, during which time substantial amounts of ash were emitted from the vent (Table 1). After 36 h, seismic records indicate a transition from discrete earthquakes to continuous volcanic tremor (Pozgay et al., 2003). Analysis of a sequence of eruption deposits on the western side of the island, and COSPEC measurements of elevated SO_2 fluxes on May 21, led Fischer et al. (2003) to conclude that the initial phreatic eruption quickly became magmatic, erupting juvenile magmas from an early stage of the eruption.

A lava dome was first sighted on June 4 (Smithsonian Institution, 2003b). However, the high heat flux values calculated from MODIS after May 17 are consistent with the presence of, in one form or another, active lava in the vent, rather than simple venting of ash and gas, which is too cool to produce thermal signals resolvable in coarse resolution satellite data (Wright et al., 2002b). This observation supports the observation of Fischer et al. (2003) that the eruption had entered its magmatic phase by May 21.

The last MODVOLC detection event occurred at 01:44 on May 29, 2003. The detection limit of the MODVOLC algorithm can be stated as a radiator with a size and surface temperature configuration that yields a power loss of 10–20 MW. To place this in context, the algorithm regularly detects the lava-lake at Mount Erebus, in Antarctica, which has recently varied between 5 and 15 m in diameter (Aster et al., 2003). The dome, as observed on June 4, was therefore too "cool" to trigger the MODVOLC alert threshold. Although destroyed by two explosions on June 16, it appears, from seismic records that indicate only continuous tremor (Smithsonian Institution, 2003b), that no explosions occurred at the dome between June 4 and June 12. As we describe in the next section, satellite data reveal that the SO_2 flux from the volcano declined steadily after May 30. If the decreasing SO_2 flux was indicative of an absence of high temperature fumaroles on the dome surface, and its cooling carapace was not being disrupted by explosions, it seems that the extruded dome was simply cooling within the crater, explaining why it did not produce significant thermal anomalies.

3.2. Satellite observations of SO_2 emissions and ash plumes during the eruption

The first unequivocal satellite-based observation of an ash plume over the volcano was reported by the Washington VAAC on May 10 at 22:32 (Smithsonian Institution, 2003a). Plume heights during the explosive phase of the eruption reportedly reached ~10–15 km (Smithsonian Institution, 2003a) and the eruption was complex, involving multiple clouds emplaced at a range of altitudes. The emissions from Anatahan traversed busy air routes (e.g., Tokyo to Sydney) and arguably the most significant hazard resulting from the eruption was ash in the path of the ~25,000 commercial aircraft that fly over the Mariana Islands annually. Here, we document observations of ash and sulphur dioxide (SO_2) emissions from Anatahan made by four polar-orbiting satellite sensors, the Earth Probe Total Ozone Mapping Spectrometer (EP TOMS), MODIS on EOS Terra and Aqua, and the Atmospheric Infrared Sounder (AIRS) on EOS Aqua, covering the period May 10–June 13, 2003.

Observations made by the four instruments are listed chronologically in Table 1, with estimates of SO_2 and ash cloud mass in kilotons. EP TOMS is an ultraviolet (UV) sensor with low-spatial-resolution (39 km at nadir), capable of measuring volcanic SO_2 and ash emissions. It is restricted to daytime operation and, in May–June 2003, incomplete coverage at low latitudes resulted in EP TOMS data gaps over the Mariana Islands on alternate days. A technical fault on the spacecraft from May 15–23 inclusive also impeded tracking of the Anatahan eruption (Table 1). Descriptions of the instrument and the techniques used to retrieve SO_2 concentrations from TOMS data

can be found in Krueger et al. (1995) and Carn et al. (2003). The infrared (IR) sensors (MODIS and AIRS) also have channels sensitive to SO_2 and ash (at 7.3 μm and 10–12 μm, respectively), and they provide better temporal and spatial resolution than EP TOMS, with a total of at least three overpasses of MODIS or AIRS per day for May 10–13, 2003. IR retrieval methods for SO_2 employed in this study are described in Carn et al. (2005) and Prata et al. (submitted for publication); the methods used for detecting ash are described in Prata (1989). SO_2 and ash column amounts derived from IR data are sensitive to the assumed altitude of the cloud; for this study, we have placed the cloud at 12 km for MODIS retrievals and at 8–13.5 km for AIRS retrievals. IR data after May 14 were not analyzed for this paper, but daily ash cloud movements derived from IR GOES data are fully documented by the Washington VAAC (http://www.ssd.noaa.gov/VAAC/anat.html).

3.3. The explosive eruption phase, May 10–12, 2003

No emissions were detected in the EP TOMS overpass of Anatahan at 11:16 on May 10, several hours before the reported eruption onset. At 23:10, a MODIS image showed large SO_2 and ash clouds in the vicinity of Anatahan (Table 1), indicative of a magmatic eruption in progress. Pronounced separation of the SO_2 and ash clouds was evident in MODIS and AIRS data at this stage, with the bulk of the ash emissions (with small amounts of SO_2) extending west of the Marianas while the higher-altitude SO_2 cloud (which also contained some ash) was carried south–southeast of Anatahan (Fig. 4). Washington VAAC estimates suggested a height of 14–15 km for the latter cloud, which was probably the highest altitude reached by any of the Anatahan emissions during the 2003 eruption. Separation of ash and SO_2 clouds is a common feature of explosive eruptions, and may be the result of rapid sedimentation of ash particles to lower altitudes or perhaps a pre-eruptive stratification of the volcano's plumbing system, with an upper, volatile-rich pocket above the magma chamber.

MODIS, AIRS and EP TOMS tracked the SO_2 cloud as it moved south of Anatahan and then east of the Marianas, with the most distant observation made by AIRS at 01:00 on May 12 when the eastern edge of the SO_2 cloud was located at 18.5°N, 163.2°E (~1900 km east of Anatahan). Elevated SO_2 concentrations continued to be detected by EP TOMS and AIRS on May 11–12 in a region extending ~1100 km from a point ~510 km west of Anatahan to a point ~700 km southeast of it (Table 1). It is unclear whether this SO_2 represented a dispersing portion of the SO_2 cloud discharged on May 10, or whether it was the product of another explosive event or vigorous gas venting from Anatahan following the initial eruption. Cloud mass estimates from EP TOMS (Table 1) suggest that the observed SO_2 contained a significant 'fresh' component. Ash emissions continued to be tracked westwards towards the Philippines from May 10 to 13 and ash was detected ~1900 km west of Anatahan by AIRS at 14:12 on May 13.

Data from the single seismometer present on Anatahan during the eruption indicate that tremor increased rapidly at 17:00–18:00 on May 10, corresponding to the onset of gas and ash emissions (Smithsonian Institution, 2003b). Tremor increased further from 10:00 until early afternoon on 11 May, remained high for a couple of days, then decreased by ~50% by May 20 (Smithsonian Institution, 2003b). The high tremor phase on May 11–12 most likely involved vigorous emission of gas (and relatively little ash) that produced the SO_2 cloud seen by EP TOMS and AIRS on those days (Table 1).

3.4. Continuous emissions, May 13–June 13, 2003

Following the explosive phase of the eruption, EP TOMS began to detect SO_2 plumes emerging from Anatahan on May 14, continuing on May 24 after the temporary instrument shutdown (Table 1). Emissions at the Washington VAAC height assignment of ~3–6 km given for these plumes would usually elude detection by EP TOMS but the sensor is capable of measuring non-eruptive degassing if SO_2 concentrations are very high (e.g., Carn, 2003). During the continuous emission phase SO_2 was rarely tracked for more than 1 day, implying a short residence time, and winds shifted regularly, dispersing the emissions in varying directions. Plume transport was affected by the passage of Typhoon Chan-hom east of the Marianas on May 20–25, which blew ash and gas south towards Saipan, Tinian, Rota and Guam (e.g., on May 24; Table 1). Otherwise, the observed plumes

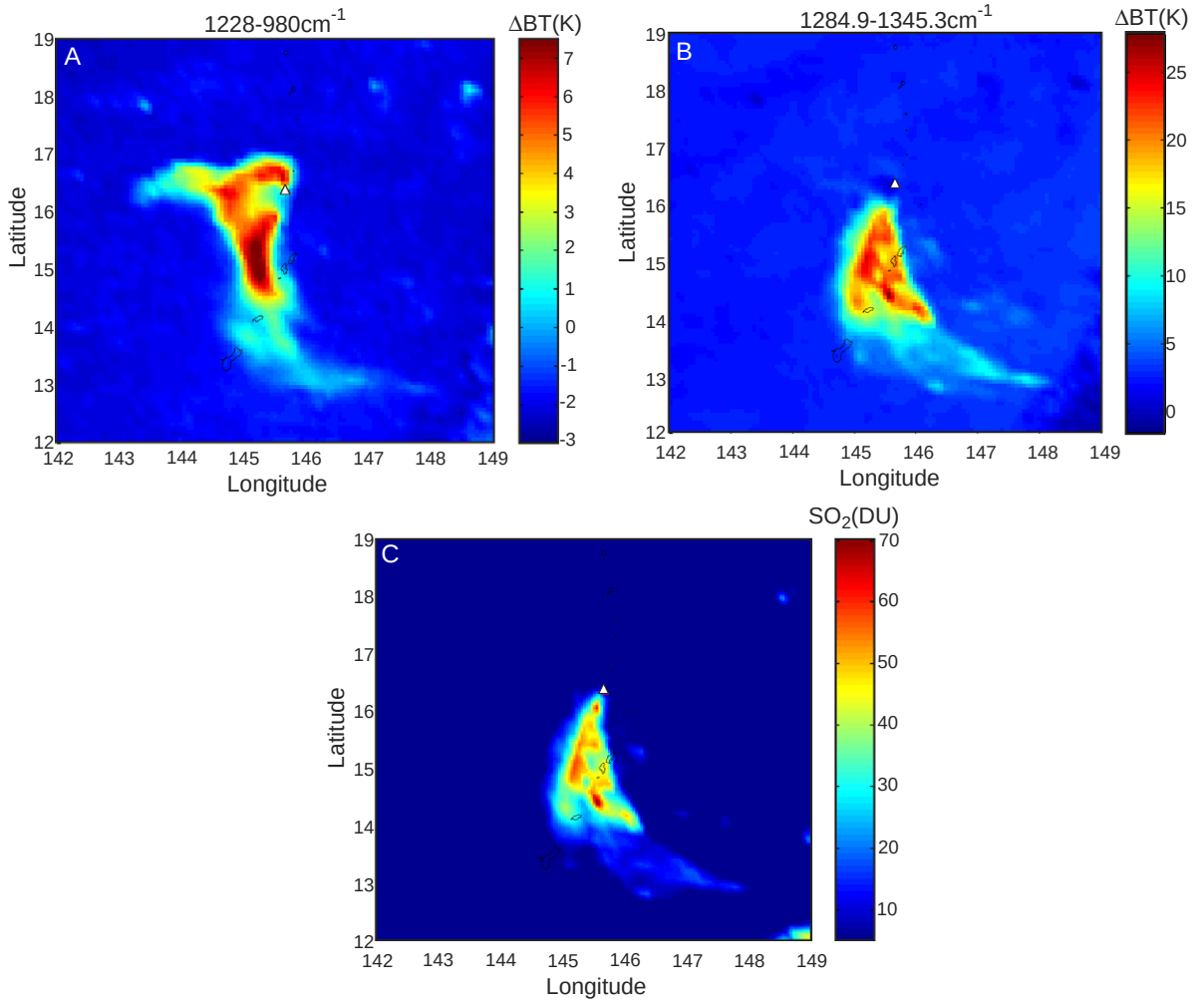

Fig. 4. AIRS images of the Anatahan eruption cloud on May 11, 2003 at 00:55; the white filled triangle marks the location of Anatahan. (A) Bias difference image showing the ash cloud, generated by calculating the brightness temperature (BT) difference between the observed AIRS BTs (containing the volcanic signal) and BTs generated from European Center for Medium range Weather Forecasting (ECMWF) model data (in which the volcanic signal is absent), and then finding the difference in this bias between two AIRS channels: one sensitive to ash (980 cm^{-1}) and the other insensitive (1228 cm^{-1}). The larger the bias difference, the stronger the volcanic signal; (B) bias difference image showing the SO_2 cloud, using AIRS channels at 1284.9 and 1345.3 cm^{-1}; (C) SO_2 retrieval image, showing SO_2 column density in milli atm cm or Dobson Units. Although the two species overlap, there is clear separation between SO_2-rich and ash-rich areas of the volcanic cloud.

were generally not directed towards other islands and dispersed west of the Marianas.

Emissions of SO_2 measured by EP TOMS seemed to decline prior to June 4, when a lava dome was first sighted, and reached a low point on June 5 (Table 1), indicating that an emerging dome may have plugged the conduit and inhibited degassing. Increased degassing apparent during May 24–30 (Table 1) may therefore relate to magma rising in the conduit and/or dome extrusion. Similar patterns were observed in SO_2 emissions at Pinatubo during pre-paroxysmal dome growth prior to the June 1991 eruption (Daag et al., 1996). However, we stress that MODVOLC data indicate the possible presence of active lava at the surface as early as May 17, so the precise chronology remains ambiguous, in part because coincident TOMS data were unavailable from May 15–23.

The Anatahan lava dome observed on June 4 was largely destroyed by two strong explosions on June 14, and after June 16 tremor dropped to a low level (Smithsonian Institution, 2003b), which is consistent with an absence of EP TOMS observations of SO_2 after mid-June (Table 1). The last space-based observation of emissions from Anatahan in 2003 was filed by the Washington VAAC on July 16 (http://www.ssd.noaa.gov/VAAC/ARCH03/archive.html).

On several occasions during the continuous emission phase, EP TOMS did not detect measurable SO_2 until the plume had traveled some distance downwind and risen to an appropriate altitude. This could be a simple effect of cloud altitude on satellite retrievals, or it could indicate release of hydrogen sulfide (H_2S) from the volcano, which was then oxidized to SO_2 during transport. A 'rotten egg' smell, characteristic of H_2S, was reported in Saipan on May 23–24 (Smithsonian Institution, 2003a) and, on May 25, the highest SO_2 column amounts measured by EP TOMS were located at the distal end of the plume, which could indicate H_2S oxidation.

An estimate of total SO_2 production by Anatahan for May 10–June 13, 2003 has been deduced using available satellite data and a COSPEC traverse conducted on May 21, which yielded an SO_2 flux of 3000–4500 t day^{-1} (Smithsonian Institution, 2003a). Using the daily satellite observations in conjunction with reasonable estimates of SO_2 amounts leftover from the preceding day, and using the COSPEC measurement and linear interpolation between data points to fill the EP TOMS data gaps, we arrive at a total SO_2 discharge of ~0.51 Mt for the ~1 month of activity, of which ~0.11 Mt was emitted during activity on May 10–12. In view of the non-ideal measurement conditions and the difficulty in accounting for data gaps, the error on this figure is probably ± 50%. Emissions between the EP TOMS shutdown on May 15 and the COSPEC deployment on May 21 are particularly uncertain, which is unfortunate given the high thermal flux measured in that period (Fig. 3B).

4. Satellite thermal observations of lava dome growth during 2004

Following the explosions that partially destroyed the dome on June 16, 2003, seismicity decreased significantly, and steam plumes, but no ash emissions, were observed thereafter (Smithsonian Institution, 2003c). This level of activity persisted until the end of the year (Smithsonian Institution, 2004).

No MODIS thermal alerts were detected during this period, although one nighttime ASTER image was acquired on November 8, 2003 (Fig. 5). Unlike the ASTER images acquired prior to the 2003 eruption image, a geothermal anomaly is evident in the eastern caldera. However, it is quite weak, with a temperature, integrated over the 90 m image pixel, of 31 °C, only 9 °C greater than the surrounding pixels. The fact that the heat source was too cool to produce a resolvable signal in ASTER's short-wave infrared wavebands, even though they have a spatial resolution of 30 m, indicates an absence of material at or near eruption temperature (Wright et al., 1999). Field reports confirm that geothermal activity within the crater during October 2003 was limited to boiling mud pools and mini-geysers (Smithsonian Institution, 2004). The small areal extent and low temperature of the volcanic activity at this time explains why the MODVOLC algorithm did not detect it.

Low levels of activity persisted until February 2004, during which two periods of heightened seismicity were recorded. A seismic swarm began beneath Anatahan on March 31, 2004 and, on April 6–7, seismicity increased to its highest level since the May–June 2003 eruption (Smithsonian Institution, 2004). At

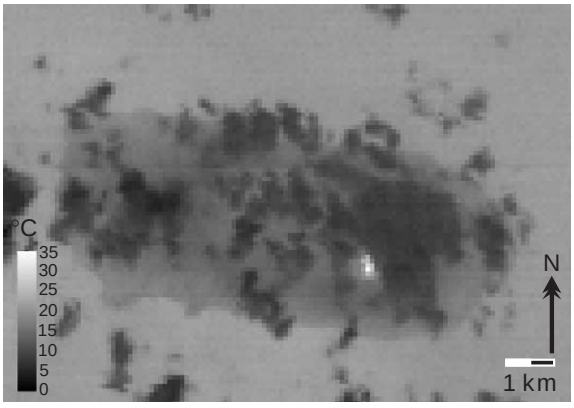

Fig. 5. Nighttime ASTER images acquired at 22:37 on November 8, 2003. Spectral radiance data at 11.318 μm (ASTER band 14) have been converted to brightness temperature, in °C. Pixel size is 90 m. Bright pixels in the eastern crater correspond to low temperature geothermal activity.

01:44 on April 13, 2004, MODVOLC detected the first hot-spot at Anatahan since the end of May 2003, located in the vicinity of the eastern caldera (Fig. 6). An over-flight on April 11 confirmed the presence of a new lava dome in the eastern caldera crater lake.

Between April 13 and June 30, 2004, MODVOLC detected hot-spots on 19 separate occasions revealing that, once more, the activity is concentrated in the eastern caldera (Fig. 6A). The thermal emission signature from the dome shows a

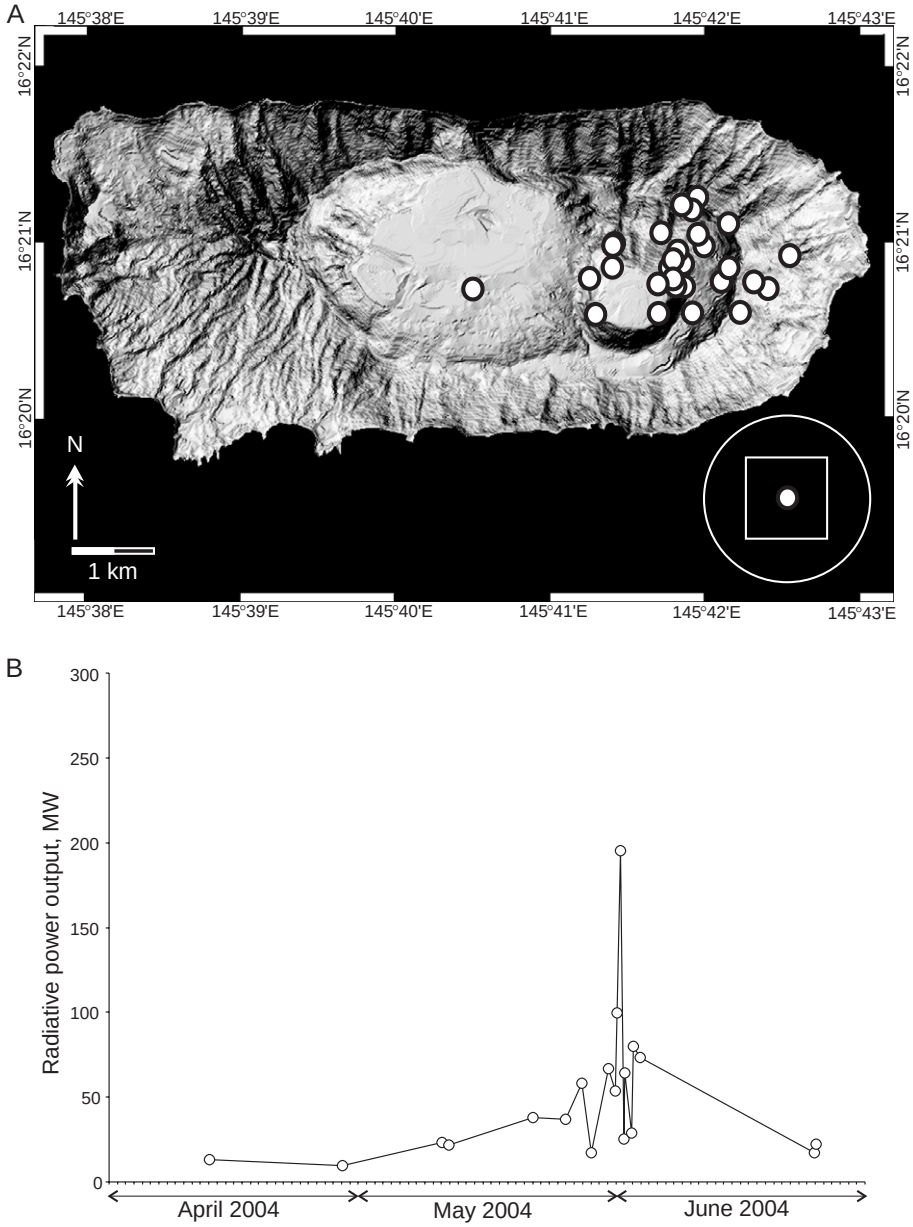

Fig. 6. (A) The spatial distribution of hot-spots detected by MODIS during the period April 1 to June 30, 2004. Each filled white circle corresponds to the center-point of the 1-km MODIS pixel that contained the hot-spot. (B) The total heat radiated by these hot-spots over the same time period.

symmetric waxing and waning character; however, the level of thermal emission during the current period of activity is, so far, substantially lower than that observed during the May–June 2003 eruption (Fig. 6B).

5. Conclusions

The May 2003 eruption of Anatahan provides a useful example of how satellite resources can be employed in near-real-time to derive quantitative volcanic eruption parameters, as well as basic information regarding the nature and distribution of the erupted products, at remote and inaccessible volcanoes.

The routine surveillance of erupting volcanoes from space is, primarily, conducted by low-spatial-resolution satellites, whose primary function is to collect meteorological, climatological and environmental data. These sensors not only have a high revisit frequency, allowing the same point on the Earth's surface to be viewed daily, but also have 100% duty cycles and, therefore, provide full coverage for all of the Earth's sub-aerially active volcanoes. While high-spatial-resolution visible, shortwave infrared and long-wave infrared data are routinely acquired for volcanoes such as Mount Etna and Kilauea, they are not for most other volcanoes. Such data sets are, however, an important complement to the more ubiquitous data sets provided by low-spatial-resolution sensors such as MODIS and AVHRR (e.g., Ramsey and Dehn, 2004). Increasingly, systems are being established which use low-spatial, but high-temporal, resolution observations of volcanic unrest, such as those provided by MODVOLC, to act as triggering mechanisms for automatic tasking of high-resolution imaging systems. In this way, high-resolution imaging sensors, such as the Earth Observing-1 Hyperion, which do not routinely acquire data for all of Earth's potentially active volcanoes, can be automatically re-tasked to acquire an image of an erupting volcano at the first available opportunity (Davies et al., 2003). As a result, in the future, more comprehensive suites of high- and low-resolution satellite data should be available to complement ground-based observations of sub-aerial eruptions.

Acknowledgments

This work was supported by NASA grant NNG04G064G. We thank Eric Pilger for maintaining the HIGP MODVOLC data base. Larrabee Strow and the AIRS Science Team at UMBC are acknowledged for developing the AIRS retrieval schemes used in this study. Scott Rowland kindly provided the Anatahan DEM. We thank Rosalind Helz (USGS) and Bill Rose (MTU) for reviewing the paper. HIGP publication number 1385 and SOEST publication number 6587.

Appendix A. Estimating radiative power loss from MODIS hot-spot pixels

The spectral radiance emitted by the hot-spot pixel at 3.959 μm ($L_{3.959}$) can be converted to an estimate of radiative power loss from that pixel (E_f in MW) by using the following approximation (Kaufman et al., 1998):

$$E_f = 4.34 \times 10^{-19}\left(T_{4h}^8 - T_{4b}^8\right). \quad \text{(A1)}$$

Here, T_{4h} (in K) is obtained by converting the measured 3.959 μm hot-spot pixel radiance value, $L_{3.959}$, to temperature by using Planck's blackbody radiation law, and T_{4b} is the temperature of the ground surrounding the volcanic heat source obtained from pixels surrounding the hot-spot pixel. We calculated E_f for each hot-spot pixel detected, at each observation time, at Anatahan. T_{4h} was obtained primarily by using band 22, which has a higher radiometric precision than band 21, although both detect radiance over the same spectral interval. However, when the emitted radiance exceeded the upper measurement limit of the band 22 detectors, band 21 data were used. Band 21 has a much larger measurement range.

Although Kaufman et al. (1998) calculated T_{4b} from the 3.959 μm radiance emitted by pixels surrounding the hot-spot pixel, MODVOLC only records the spectral radiance emitted by the hot-spot pixels themselves. However, it can be shown (Wright et al., 2002a) that the band 32 (12.02 μm) temperatures of the hot-spot pixels, which MODVOLC does record, can be used to obtain an estimate for T_{4b}.

We use the method described by Wright and Flynn (2004) with two exceptions. Firstly, we use the median band 32 hot-spot temperature recorded at Anatahan during each month to obtain T_{4b}, rather than the minimum. We do this to avoid using anomalously low 12.02 μm temperatures, for example, those that may result when a sub-pixel-sized hot-spot is partially obscured by cold meteorological clouds. Secondly, we used nighttime and daytime MODIS data to compute the radiant heat flux curves shown in Figs. 3 and 6. During the day, the Earth both emits and reflects electromagnetic radiation at 3.959 μm. As a result, raw bands 21 and 22 radiances ($L_{3.959}$) must be corrected for the reflected sunlight component before they are converted to temperatures for use in Eq. (A1) or anomalously high heat fluxes will result. Assuming that by day the radiance recorded at 1.6 μm ($L_{1.6}$) is purely reflected light (appropriate at these coarse spatial resolutions; see Wooster and Rothery, 1997) and that the amount of energy reflected by the hot-spot pixel at 3.959 μm is equivalent to 4.26% of that reflected at 1.6 μm (based on the top-of-the-atmosphere solar irradiance), we estimate the spectral radiance at 3.959 μm due to thermal emission from the hot-spot, $L_{3.959(\mathrm{corr})}$, using:

$$L_{3.959(\mathrm{corr})} = L_{3.959} - (0.0426 \times L_{1.6}). \quad \text{(A2)}$$

We then use $L_{3.959(\mathrm{corr})}$ as the basis for estimating the radiative power loss from hot-spot pixels observed during the day.

References

Aster, R., Mah, S., Kyle, P., McIntosh, W., Dunbar, M., Johnson, J., Ruiz, M., McNamara, S., 2003. Very long period oscillations of Mount Erebus volcano. J. Geophys. Res. 108, B11. doi:10.1029/2002JB002101.

Carn, S.A., 2003. Eruptive and passive degassing of sulfur dioxide at Nyiragongo volcano (D.R. Congo): the 17 January eruption and its aftermath. Acta Vulcanol. 15, 75–86.

Carn, S.A., Krueger, A.J., Bluth, G.J.S., Schaefer, S.J., Krotkov, N.A., Watson, I.M., Data, S., 2003. Volcanic eruption detection by the Total Ozone Mapping Spectrometer (TOMS) instruments: a 22-year record of sulphur dioxide and ash emissions. In: Oppenheimer, C., Pyle, D.M., Barclay, J. (Eds.), Volcanic Degassing. Geol. Soc. London Spec. Publ., vol. 213. pp. 177–202.

Carn, S.A., Strow, L.L., de Souza-Machado, S., Edmonds, Y., Hannon, S., 2005. Quantifying tropospheric volcanic emissions with AIRS: the 2002 eruption of Mt. Etna (Italy). Geophys. Res. Lett. 32, L02301. doi:10.1029/2004GL021034.

Daag, A.S., Tubianosa, B.S., Newhall, C.G., Tuñgol, N.M., Javier, D., Dolan, M.T., Delos Reyes, P.J., Arboleda, R.A., Martinez, M.M.L., Regalado, M.T.M., 1996. Monitoring sulfur dioxide emission at Mount Pinatubo. In: Newhall, C.G., Punongbayan, R.S. (Eds.), Fire and Mud: Eruptions and Lahars of Mount Pinatubo, Philippines. University of Washington Press, Seattle, WA, pp. 409–414.

Davies, A.G., Chien, S., Wright, R., Cervelli, P., Flynn, L.P., Baker, V., Castano, R., Cichy, B., Dohn, J., Doggett, T., Greeley, R., Sherwood, R., Williams, K., Frye, S., Kones, J., 2003. Streamlining spacecraft observation response to volcanic activity detection with a ground and space-based sensorweb system. EOS Trans. Fall Meet. Suppl., Abstract, V51F-0347.

Fischer, T.P., Hilton, D.R., DeMoor, J., Jaffe, L., Spilde, M.N., Counce, D., Comacho, J.T., 2003. The first historical eruption of Anatahan volcano, Mariana Islands. EOS Trans. Fall Meet. Suppl., Abstract, V32B-1009.

Flynn, L.P., Harris, A.J.L., Wright, R., 2001. Improved identification of volcanic thermal features using Landsat 7 ETM+. Remote Sens. Environ. 78, 180–193.

Kaufman, Y.J., Justice, C.O., Flynn, L.P., Kendall, J.D., Prins, E.M., Giglio, L., Ward, D.E., Menzel, W.P., Setzer, A.W., 1998. Potential global fire monitoring from EOS-MODIS. J. Geophys. Res. 103, 32215–32238.

Krueger, A.J., Walter, L.S., Bhartia, P.K., Schnetzler, C.C., Krotkov, N.A., Sprod, I., Bluth, G.J.S., 1995. Volcanic sulfur dioxide measurements from the Total Ozone Mapping Spectrometer instruments. J. Geophys. Res. 100 (D7), 14057–14076.

Pieri, D.C., Abrams, M., 2004. ASTER watches the world's volcanoes: a new paradigm for volcanological observations from orbit. J. Volcanol. Geotherm. Res. 135, 13–28.

Pozgay, S.H., Wiens, D.A., Shore, P.J., Sauter, A., Comacho, J.T., 2003. Seismic recording of the Anatahan eruption. EOS Trans. Fall Meet. Suppl., Abstract, V32B-1019.

Prata, A.J., 1989. Observations of volcanic ash clouds in the 10–12 micrometer window using AVHRR/2 data. Int. J. Remote Sens. 10, 751–761.

Prata, A.J., Watson, I.M., Rose, W.I., O'Brien, D.M., Realmuto, V.J., Bluth, G.J.S., Servranckx, R., Crisp, J., submitted for publication. Volcanic sulphur dioxide concentrations derived from infrared satellite measurements. J. Geophys. Res.

Ramsey, M., Dehn, J., 2004. Spaceborne observations of the 2000 Bezymianny, Kamchatka eruption: the integration of high-resolution ASTER data into near real-time monitoring using AVHRR. J. Volcanol. Geotherm. Res. 135, 127–146.

Rothery, D.A., Oppenhemier, C., Bonneville, A., 1995. Infrared thermal monitoring. In: McGuire, B., Kilburn, C.R.J., Murray, J.B. (Eds.), Monitoring Active Volcanoes. UCL Press, London, pp. 184–216.

Smithsonian Institution, 1990. Anatahan. Bull. Glob. Volcanism Netw. 15 (3), 5.

Smithsonian Institution, 2003a. Anatahan. Bull. Glob. Volcanism Netw. 28 (5), 2–5.

Smithsonian Institution, 2003b. Anatahan. Bull. Glob. Volcanism Netw. 28 (6), 10–11.

Smithsonian Institution, 2003c. Anatahan. Bull. Glob. Volcanism Netw. 28 (9), 4.

Smithsonian Institution, 2004. Anatahan. Bull. Glob. Volcanism Netw. 29 (4), 7–9.

Watson, I.M., Realmuto, V.J., Rose, W.I., Prata, A.J., Bluth, G.J.S., Gu, Y., Bader, C.E., Yu, T., 2004. Thermal infrared remote sensing of volcanic emission using the moderate resolution imaging spectroradiometer. J. Volcanol. Geotherm. Res. 135, 75–89.

Wolfe, R.E., Nishihama, M., Fleig, A.J., Kuyper, J.A., Roy, D.P., Storey, J.C., Patt, F.S., 2002. Achieving sub-pixel geolocation accuracy in support of MODIS land science. Remote Sens. Environ. 83, 31–49.

Wooster, M.J., Rothery, D.A., 1997. Thermal monitoring of Lascar volcano, Chile, using infrared data from the along-track scanning radiometer: a 1992–1995 time series. Bull. Volcanol. 58, 566–579.

Wright, R., Flynn, L.P., 2004. Space-based estimate of the volcanic heat flux into the atmosphere during 2001 and 2002. Geology 32, 189–192.

Wright, R., Flynn, L.P., 2003. Satellite observations of thermal emission before, during, and after the January 2002 eruption of Nyiragongo. Acta Vulcanol. 15, 67–74.

Wright, R., Rothery, D.A., Blake, S., Harris, A.J.L., Pieri, D.C., 1999. Simulating the response of the EOS Terra ASTER sensor to high-temperature volcanic targets. Geophys. Res. Lett. 26, 1773–1776.

Wright, R., Flynn, L.P., Garbeil, H., Harris, A.J.L., Pilger, E., 2002a. Automated volcanic eruption detection using MODIS. Remote Sens. Environ. 82, 135–155.

Wright, R., De La Cruz-Reyna, S., Harris, A.J.L., Flynn, L.P., Gomez-Palacios, J.J., 2002b. Infrared satellite monitoring at Popocatépetl: explosions, exhalations, and cycles of dome growth. J. Geophys. Res. 107. doi:10.1029/2000JB000125.

Wright, R., Flynn, L.P., Garbeil, H., Harris, A.J.L., Pilger, E., 2004. MODVOLC: near-real-time thermal monitoring of global volcanism. J. Volcanol. Geotherm. Res. 135, 29–49.